Scientific Research Report

Diabetic Macrophage Exosomal miR-381-3p Inhibits Epithelial Cell Autophagy Via NR5A2

Xin Huang [a,#], *Linhesheng Wei* [a,#], *Mengdi Li* [b], *Yong Zhang* [a], *Shuhong Kuang* [a], *Zongshan Shen* [a], *Hui Liu* [a], *Zhengmei Lin* [a*]

[a] *Hospital of Stomatology, Guangdong Provincial Key Laboratory of Stomatology, Guanghua School of Stomatology, Sun Yat-sen University, Guangzhou, Guangdong, China*

[b] *Department of Periodontology, Shanghai Ninth People's Hospital, Shanghai Jiao Tong University School of Medicine, College of Stomatology, Shanghai Jiao Tong University, National Center for Stomatology, National Clinical Research Center for Oral Diseases; Shanghai Key Laboratory of Stomatology, Shanghai Research Institute of Stomatology, Shanghai, China*

ARTICLE INFO

Article history:
Received 5 November 2023
Received in revised form
12 January 2024
Accepted 2 February 2024
Available online 28 April 2024

Key words:
Diabetic Periodontitis
Autophagy Flux
NR5A2
miR-381-3p
Macrophage Epithelial Cell Interaction

ABSTRACT

Purpose: To explore the mechanism underlying autophagy disruption in gingival epithelial cells (GECs) in diabetic individuals.

Methods and materials: Bone marrow-derived macrophages (BMDMs) and GECs were extracted from C57/bl and db/db mice, the exosomes (Exo) were isolated from BMDMs. qRT–PCR and Western blotting were performed to analyse gene expression. The AnimalTFDB database was used to identify relevant transcription factors, and miRNA sequencing was utilised to identify relevant miRNAs with the aid of the TargetScan/miRDB/miRWalk databases. A dual-luciferase assay was conducted to verify intermolecular targeting relationships.

Results: Similar to BMDMs, BMDM-derived Exos disrupted autophagy and exerted proinflammatory effects in GEC cocultures, and ATG7 may play a vital role. AnimalTFDB database analysis and dual-luciferase assays indicated that NR5A2 is the most relevant transcription factor that regulates *Atg7* expression. SiRNA-NR5A2 transfection blocked autophagy in GECs and exacerbated inflammation, whereas NR5A2 upregulation restored ATG7 expression and ameliorated Exo^{DM}-mediated inflammation. MiRNA sequencing, with TargetScan/miRDB/miRWalk analyses and dual-luciferase assays, confirmed that miR-381-3p is the most relevant miRNA that targets NR5A2. MiR-381-3p mimic transfection blocked autophagy in GECs and exacerbated inflammation, while miR-381-3p inhibitor transfection restored ATG7 expression and attenuated Exo^{DM}-mediated inflammation.

Conclusion: BMDM-derived Exos, which carry miR-381-3p, inhibit NR5A2 and disrupt autophagy in GECs, increasing periodontal inflammation in diabetes.

Introduction

The gingival epithelium plays an important role as a barrier against oral bacteria, and this barrier depends on normal systemic and local immunity. Type II diabetes mellitus is a chronic metabolic disorder that affects 537 million people worldwide,[1] and it is characterised by chronic hyperglycaemia and systemic inflammation. Uncontrolled hyperglycaemia can exacerbate periodontal inflammation, leading to rapid alveolar bone absorption and eventual tooth loss, which are largely attributed to the abnormal innate immune

Abbreviations: GECs, gingival epithelial cells; NLRP3, NACHT, LRR, and PYD domain-containing protein 3; Exos, Exosomes; BMDMs, bone marrow-derived macrophages

* *Corresponding author*. Hospital of Stomatology, Guangdong Provincial Key Laboratory of Stomatology, Guanghua School of Stomatology, Sun Yat-sen University, Guangzhou, Guangdong, China.
E-mail address: linzhm@mail.sysu.edu.cn (Z. Lin).
Xin Huang: http://orcid.org/0000-0001-9924-1055
Yong Zhang: http://orcid.org/0000-0002-5438-130X
Shuhong Kuang: http://orcid.org/0000-0002-8439-913X
Hui Liu: http://orcid.org/0000-0003-2200-0063

Xin Huang and Linhesheng Wei contribute equally to this study.

https://doi.org/10.1016/j.identj.2024.02.001

responses of gingival epithelial cells (GECs). The precise mechanism underlying this process is not yet fully understood.

Autophagy is a biological process that plays a key role in regulating the immune response. The formation of autophagosomes is regulated by a group of autophagy-related (ATG) proteins, and ATG8 (also known as LC3 or LC3b) is widely used as a marker of autophagy.[2] ATG3 and ATG7 act as E1 and E2 ubiquitin ligases of LC3b, respectively, and are involved in the conversion of LC3-I to LC3-II, which is the form of this protein that attaches to the autophagosome surface. Previous studies have demonstrated that the autophagy flux is disrupted under high glucose conditions, and chronic or irreversible disruption of autophagy can lead to the overexpression of the NACHT, LRR, and PYD domain-containing protein 3 (NLRP3) inflammasome. Thus, it is suggested that autophagy plays an essential role in the inflammatory state of GECs under high glucose conditions.

Macrophages play crucial roles in innate immune responses of periodontal tissues. When infection occurs, peripheral monocytes migrate to periodontal tissues, differentiate into macrophages and participate in the elimination of pathogens.[3] Studies have indicated that macrophages can alter the response of nonprofessional phagocytes (such as GECs) to inflammation by releasing vesicles.[4] Exosomes (Exos), which are extracellular vesicles that contain a large number of biochemical messengers (nucleic acids, proteins, etc.), are thought to be involved in transportation, communication and intercellular regulatory processes.[5]

However, the immunomodulatory effect of macrophages on GECs has yet to be elucidated. To investigate this, bone marrow-derived macrophages (BMDMs) and gingival epithelial cells (GECs) were derived and cultured, the Exos from BMDMs were extracted. BMDMs or BMDM-derived Exos were cocultured with GECs. Bioinformatics analysis, including miRNA sequencing, the AnimalTFDB database and TargetScan/miRWalk/miRanda databases, were conducted, dual luciferase analysis was performed. It was found that miR-381-3p from BMDMs is the key molecule that regulates NR5A2 expression in GECs, which blocks the autophagic flux and exacerbates periodontal inflammasome activation in individuals with diabetes.

Materials and methods

Ethics statement

The animals that were used in this study were obtained from the National Resource Center of Model Mice (Nanjing, China). All the experimental protocols complied with the ARRIVE guidelines and were approved by the Animal Care and Use Committee of Sun Yat-sen University (SYSU-IACUC-2019-000981).

RT–PCR analysis

Total RNA was extracted from cells using Nucleozol Reagent (Gene Company Limited, Hong Kong, China). The RNA was then reverse transcribed to generate first-strand cDNA using the PrimeScript RT Master Mix (Toyobo Co, Ltd, Osaka, Japan). The cDNA was used as a template for PCRs using the Bio-Rad CFX96 Detection System (Roche, Sweden) and SYBR PCR Master Mix (Roche, Indianapolis, IN, USA). The primers that were used are listed below (Table 1). A relative quantitative analysis was carried out to quantify the relative gene expression compared to the expression of the housekeeping gene GAPDH using a standard curve.

Table 1 – Primers used in RT–PCR analysis.

Gene	Sequence (5′ to 3′)
P62	Forward: GAACTCGCTATAAGTGCAGTGT
	Reverse: AGAGAAGCTATCAGAGAGGTGG
Nlrp3	Forward: ATCAACAGGCGAGACCTCTG
	Reverse: GTCCTCCTGGCATACCATAGA
Il-1β	Forward: GAAATGCCACCTTTTGACAGTG
	Reverse: TGGATGCTCTCATCAGGACAG
Atg3	Forward: CTGGAGATCACTTAGTCCACCA
	Reverse: GTCGGAAGATATGCCTTCACTTT
Atg7	Forward: TGACCTTCGCGGACCTAAAGA
	Reverse: CCCGGATTAGAGGGATGCTC
Lc3b	Forward: TTATAGAGCGATACAAGGGGGAG
	Reverse: CGCCGTCTGATTATCTTGATGAG
Nr5a2	Forward: TCTGAGCCATGTAGCCTTGC
	Reverse: GGAAAGTGACCATAGGGTTGGTA
Gapdh	Forward: TGACCTCAACTACATGGTCTACA
	Reverse: CTTCCCATTCTCGGCCTTG

Western blotting

Radioimmunoprecipitation assay (RIPA) buffer (Millipore, MA, USA) was used to extract proteins on ice for 30 minutes, followed by centrifugation for 15 minutes. The total protein concentrations of the lysates were then determined using the BCA protein assay kit (CWBioTech, Beijing, China). Subsequently, the proteins were separated by SDS–PAGE and transferred to polyvinylidene fluoride (PVDF) membranes (Millipore, MA, USA). The PVDF membranes were then blocked with a buffer containing 5% bovine serum albumin for 1 hour at room temperature prior to being probed with the designated primary antibodies as listed (Table 2). Then, a secondary antibody (1:1000; Abcam) was added and incubated,

Table 2 – Designated primary antibodies.

Marker (species)	Dilution	Distributor/source (catalog number)
Primary antibody:		
ATG3 rabbit pAb	1:5000	ZENBIO (383552)
ATG7 rabbit pAb	1:5000	ZENBIO (383498)
IL-1β rabbit pAb	1:1000	ZENBIO (511369)
P62 rabbit pAb	1:5000	ZENBIO (380612)
NLRP3 rabbit pAb	1:1000	ZENBIO (383319)
LC3A/B rabbit pAb	1:10000	ZENBIO (306019)
β- Tubulin mouse mAb	1:5000	ZENBIO (250007)
NR5A2 rabbit pAb	1:1000	ZENBIO (381879)
GAPDH mouse mAb	1:10000	ZENBIO (200306-7E4)
Secondary antibody:		
Anti-mouse IgG HRP-linked Ab	1:5000	CST (7076)
Anti-rabbit IgG HRP-linked Ab	1:5000	CST (7074)

and a chemiluminescence kit (Millipore) was used to visualise the results.

BMDM and GEC derivation, culture, and identification

Bone marrow cells were harvested from db/db mice by flushing their femurs, and the cells were differentiated in Dulbecco's modified Eagle's medium (DMEM/F-12; Gibco; Thermo Fisher Scientific, MA, USA) supplemented with 20% L929 supernatant containing macrophage-colony stimulating factor (M-CSF), 20% foetal bovine serum (FBS; Gibco; Thermo Fisher Scientific, USA) and 100 IU/mL penicillin/streptomycin (Sigma–Aldrich, MO, USA). After 7 days, single-cell suspensions of BMDMs were resuspended at a density of 10^6 cells/100 μL in Zombie viability dye (BioLegend, San Diego, CA, USA) and incubated for 15 minutes at room temperature to exclude dead cells from the analysis. Subsequently, the suspensions were stained with antibody against F4/80 (123115, BioLegend, San Diego, CA, USA) in the dark at 4°C for 30 minutes. Data were acquired with CytoFlex (Beckman CytoFlex, USA) and analysed using FlowJo V10.0 (Treestar, Ashland, OR, USA). The mice were euthanised with an intraperitoneal overdose of anaesthesia to ensure that they experienced no discomfort.

The isolation, processing and analysis of GECs that were harvested from C57BL mice were performed as previously described with slight modifications.[6] Briefly, the mice were euthanised, and gingival tissues were peeled from the anterior border of the maxilla bone. The gingival tissues were cut into small pieces that were 0.3 cm in diameter using a scalpel and then digested in a solution of 2 mg/mL dispase II (Sigma–Aldrich, St. Louis, MO, USA) for 8 h at 4°C. After centrifugation, the pale yellow gingival epithelium was carefully separated from the connective tissue using microscopic tweezers. The specimens were digested with 0.05% trypsin-EDTA (Invitrogen) for 15 minutes at 37°C, centrifuged, resuspended, and incubated in DMEM/F-12 (Gibco; Thermo Fisher Scientific, MA, USA) supplemented with 10% foetal bovine serum at 37°C in 5% CO_2. After 14 days of culture, cell passage was performed using 0.05% trypsin-EDTA (Invitrogen). Cells in the first or second passage were cultured for 24 hours to confirm cell attachment, and the cells were cultured for another 24 hours for the indicated experiments.

Exo extraction and identification

To harvest Exos from BMDMs, the cells were grown to 80% confluence in complete medium supplemented with 10% Exo-depleted FBS for 2 days. Exo-depleted FBS was prepared by the ultracentrifugation of FBS at 4°C and 120,000 × g for 18 hours, followed by filtration using a 0.22-μm syringe filter. Subsequently, conditioned media from BMDM cultures were centrifuged at increasing speeds to eliminate large dead cells and cell debris. The final supernatants were then ultracentrifuged at 120,000 × g for 2.5 hours at 4°C to pellet small vesicles, which corresponded to Exos. The Exo pellets were reconstituted in PBS and stored at -80°C. Flow cytometry was used to verify the presence of Exo surface markers, such as CD63 (BD Biosciences, San Jose, CA, USA, 556019, 1:1000) and CD81 (BD Biosciences, San Jose, CA, USA, 555676, 1:1000).

Transwell culture

Cocultures of BMDMs and GECs were established in a Transwell system with a 0.4 μm pore size (4×10^6 pores/cm^2). For the experiment, 2.5×10^5 GECs were seeded in the lower compartment of a 6-well Transwell system, while 2.5×10^5 BMDMs were seeded in the insert. The culture medium that was used for this experiment was DMEM supplemented with 10% Exo-depleted FBS, 100 IU/mL penicillin and 100 μg/mL streptomycin. Duplicate samples were established in each experiment, and the experiment was repeated three times. The purpose of this experiment was to test the hypothesis that BMDMs exert an effect on GECs through Exos.

Verification of Exo uptake

The uptake of Exos by GECs was assessed using a Dil staining kit (YEASEN, Shanghai, China) according to the manufacturer's instructions. One hundred microliters of purified BMDM-Exos was incubated with 5 μL of Dil for 15 minutes at 37°C, followed by ultracentrifugation at 120,000 × g for 90 minutes to remove the unbound dye. The labelled Exos were then washed twice with PBS with centrifugation at 120,000 × g, and the Exos were resuspended in PBS prior to use. Subsequently, the labelled Exos were incubated with GECs for 24 hours, and the cells were observed under a confocal microscope (Zeiss, Germany).

Exo small RNA sequencing

BMDM-derived Exos from db/db mice and C57bl mice was extracted. Total RNA was isolated by using Trizol (Invitrogen, USA). The quantity and integrity of RNA yield was assessed by using the Qubit®2.0 (Life Technologies, USA) and Agilent 2200 TapeStation (Agilent Technologies, USA) separately. 1μg total RNA of each samples were used to prepare small RNA libraries by NEBNext® Multiplex Small RNA Library Prep Set for Illumina (NEB,USA) according to manufacturer's instructions. The libraries were sequenced by HiSeq 2500 (Illumina, USA) with single-end 50bp at Ribobio Co. Ltd (Ribobio, China).

The raw reads were processed by filtering out containing adapter, poly 'N', low quality, smaller than 17nt reads by FASTQC to get clean reads. Mapping reads were obtained by mapping clean reads to reference genome of by BWA. miRDeep2 was used to identify known mature miRNA based on miRBase21 (www.miRBase.org) and predict novel miRNA. Databases of Rfam12.1 (www.rfam.xfam.org) and pirnabank (www.pirnabank.ibab.ac.in) were used to identify rRNA, tRNA, snRNA, snoRNA and piRNA by BLAST. The miRNA expression were calculated by RPM (Reads Per Million) values (PRM=(number of reads mapping to miRNA/ number of reads in Clean data) × 106).

The expression levels were normalised by RPM, RPM is equal to (number of reads mapping to miRNA/number of reads in Clean data) × 106. Differential expression between two sets of samples was calculated by edgeR algorithm according to the criteria of |log2 (Fold Change) |≥1 and *P*-value <.05.

Bioinformatics analysis

According to the AnimalTFDB database (v. 3.0), NR5A2 is the most relevant transcription factor that regulates Atg7 expression. To identify miRNAs that target NR5A2 mRNA, we used TargetScan database version 6.0 (http://www.targetscan.org/), miRWalk version 3.0 (http://mirwalk.umm.uni-heidelberg.de/) and miRanda (http://www.microrna.org/microrna/home.do). Moreover, we combined the analysis of differentially expressed miRNAs with the prediction of miRNA targets and conducted an in-depth analysis of the intersecting gene set.

Dual luciferase analysis

Two dual luciferase experiments were used in this study. One is conducted to verify the relationship between miR-381-3p and NR5A2. To this end, Nr5a2 recombinant plasmids (Nr5a2-WT and Nr5a2-Mut) and mimic NC or miR-381-3p mimic were transfected into 293T cells. The luciferase activity was then measured using a dual luciferase assay kit (Promega Corporation, Wisconsin, USA) according to the manufacturer's instructions. Another dual luciferase activity assay was conducted to verify the relationship between ATG7 and NR5A2. The sequence of the ATG7 promoter region was inserted upstream of F-Luciferase in the pGL3-basic vector, and the coding sequence of the transcription factor NR5A2 was inserted into the eukaryotic expression vector pcDNA3.1. The R-Luciferase vector (pRL-TK) was used as an internal reference, and 293T cells were cotransfected for this assay. The F-Luciferase activity was then measured using luciferase readings.

Statistical analyses

Data from at least three independent experiments are presented as the mean ± *s.d.* After testing for normality, all the data were analysed using 2-tailed unpaired Student's *t* tests or one-way ANOVA with Tukey's post hoc test. All the statistical analyses were conducted using GraphPad Prism software.

Results

Coculturing GECs with BMDMs from diabetic mice impairs the autophagic flux and exacerbates inflammation via the transmission of Exos

Infiltration and dysfunction of macrophages in the gingival epithelium of diabetic mice has been reported.[7] To further investigate this phenomenon and discern whether BMDMs may regulate GECs, bone marrow cells were isolated from mice and differentiated into macrophages, and these macrophages were identified by flow cytometry (Figure 1A). Subsequently, extracellular vesicles were purified from BMDM culture supernatants and characterised by determining Exo marker expression by flow cytometry (Figure 1B). Next, DiI-labelled Exos were cocultured with GECs, resulting in an observable amount of red fluorescence in GECs, which indicated that macrophage-secreted Exos were successfully taken up by GECs (Figure 1C).

Next, BMDMs/Exos+GECs coculture systems were established (Figure 1D), and the autophagy flux and inflammation levels were evaluated by qRT–PCR and Western blotting. Compared to the coculture system that included BMDMs from C57BL mice+GECs (GECs+BMDMs^{con} group), the mRNA expression levels of *Nlrp3, Il1β, and P62* were significantly increased and the expression levels of *Atg7* were significantly decreased in the coculture system that included BMDMs from db/db mice+GECs (GECs+BMDMs^{DM} group) (Figure 1E). Similar results were observed in the coculture system that included BMDM Exos from db/db mice+GECs (GECs+Exos^{DM} group) (Figure 1E). In comparison to the GECs+BMDMs^{con} group, the protein expression levels of NLRP3 and IL1β were significantly increased, while the LC3II/I ratio and ATG7 expression levels were decreased in the GECs+BMDMs^{DM} group (Figure 1F,G). Similar results were observed in the GECs+Exos^{DM} group (Figure 1F/G). No significant difference in the ATG3 mRNA or protein expression levels was observed between the GECs +BMDMs^{con} and GECs+BMDMs^{DM} groups (Figure 1E-G). These results suggest that BMDMs from diabetic mice can disrupt the autophagic flux and exacerbate inflammation in GECs in an Exo transmission-dependent manner, and ATG7 may play a key role.

NR5A2 is a major transcription factor that regulates the transcription of the autophagy-related protein ATG7 in GECs

Analysis of the Animal TFDB database (v. 3.0) revealed that NR5A2 is the most relevant transcription factor that regulates Atg7 expression, as indicated by the presence of four-forkhead motifs in the 1000 bp upstream sequence of the Atg7 transcription start site (Supplementary Data S1). To further investigate the binding relationship, a dual-luciferase reporter assay was conducted with mutated versions of the four-forkhead motifs (MUT1, MUT2, MUT3, and MUT4) (Figure 2A). The results showed that the luciferase activity was significantly increased in the Atg7-MUT3/Atg7-MUT4 group compared to the Atg7-WT group, suggesting that binding sites 3 and 4 were the binding targets of NR5A2 (Figure 2B).

The expression of NR5A2 in GECs from diabetic and nondiabetic mice was then measured using RT–PCR and Western blotting. Western blotting analysis revealed that the protein expression levels of NR5A2 in GECs were significantly lower in diabetic mice (Figure 2C,E). However, the mRNA expression of *Nr5a2* in GECs was not significantly different (Figure 2F). Furthermore, compared to the GECs+BMDMs^{con} group, the protein expression level of NR5A2 was downregulated in the GECs+BMDMs^{DM} and GECs+Exos^{DM} groups (Figure 2D,G), while the mRNA expression level of *Nr5a2* was not significantly altered (Figure 2H).

Collectively, these findings suggest that NR5A2 functions as a transcription factor and upregulates ATG7 expression in GECs, and its protein expression is downregulated at the posttranscription level in the GECs of individuals with diabetes. It is likely that in individuals with diabetes, BMDMs play a key role in regulating the protein expression of NR5A2 in GECs via Exo transmission.

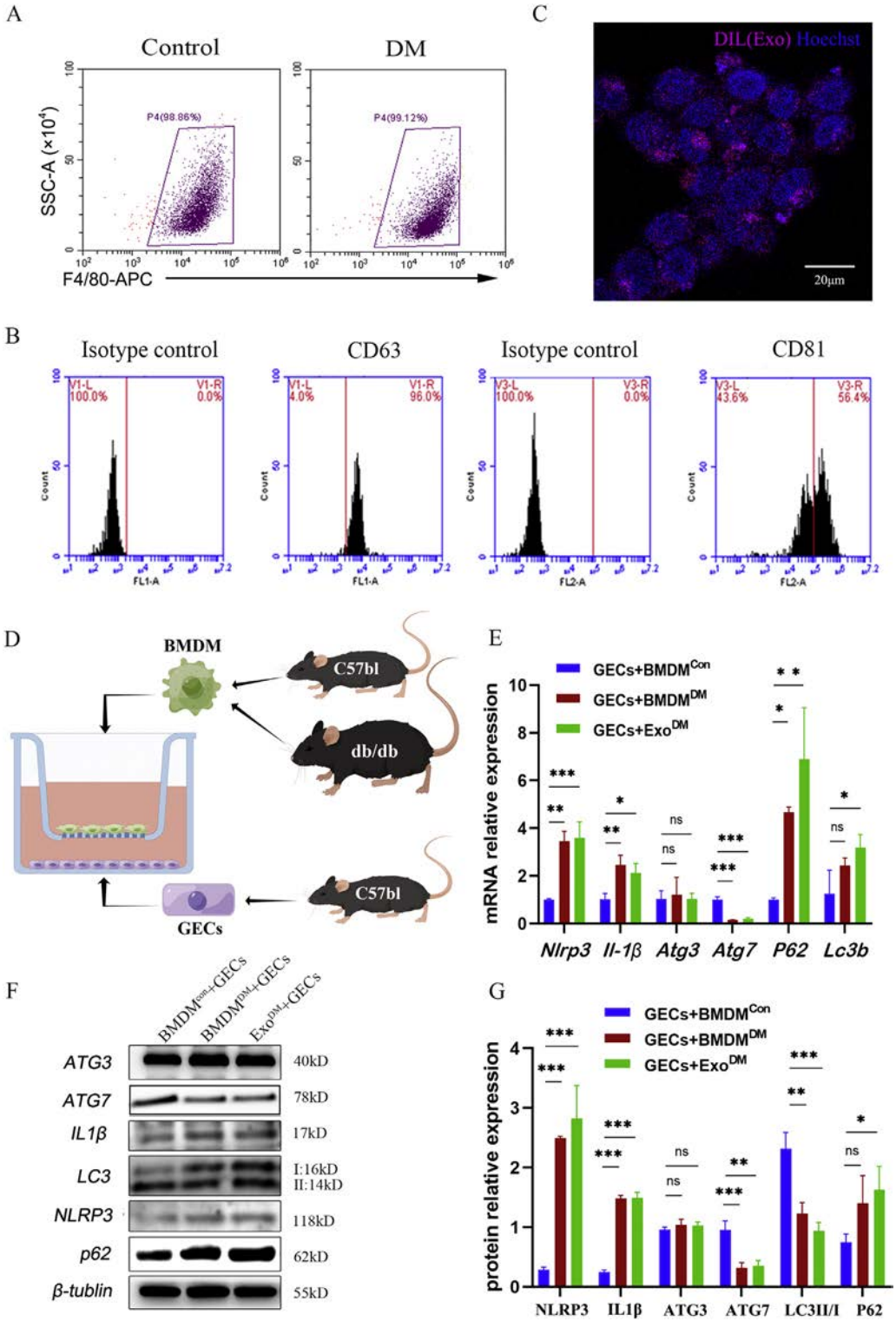

Fig. 1 – Macrophages disrupt the autophagic flux and enhance inflammation in the gingival epithelium in an Exo transmission-dependent manner. A, The purity of BMDMs was determined by staining with an anti-F4/80 antibody and flow cytometry. B, Representative fluorescence microscopic images of the Exo uptake assay. Scale bar: 20 μm. Merged images of Exos and cells showed that DIL-labelled BMDMs/Exos (red) were incorporated into Hoechst-labelled GECs (green). C, Expression of extracellular vesicle markers (CD63 and CD81) was measured by flow cytometry. D, Schematic diagram of the Transwell assay with BMDMs and GECs (By Figdraw). E, qRT–PCR was used to analyse the effect of BMDMs and BMDMs/Exos on the autophagic flux (autophagy genes: *Atg3*, *Atg7*, *Lc3b*, and *p62*) and inflammation levels (inflammatory genes: *Nlrp3* and *Il-1β*) in GECs. F and G, Western blotting was used to analyse the autophagic flux and inflammation levels in GECS after they were incubated with BMDMs and BMDMs/Exos (F), and statistical analysis was performed. G, All the Western blotting and quantitative RT–PCR experiments were repeated three independent times ($n = 3$), $^{*}P < .05$ $^{**}P < .01$ $^{***}P < .001$. The data are shown as the mean ± *s.d.* DM: harvested from db/db mice; Con: harvested from C57BL mice; Exo: Exosome secreted by bone marrow-derived macrophages.

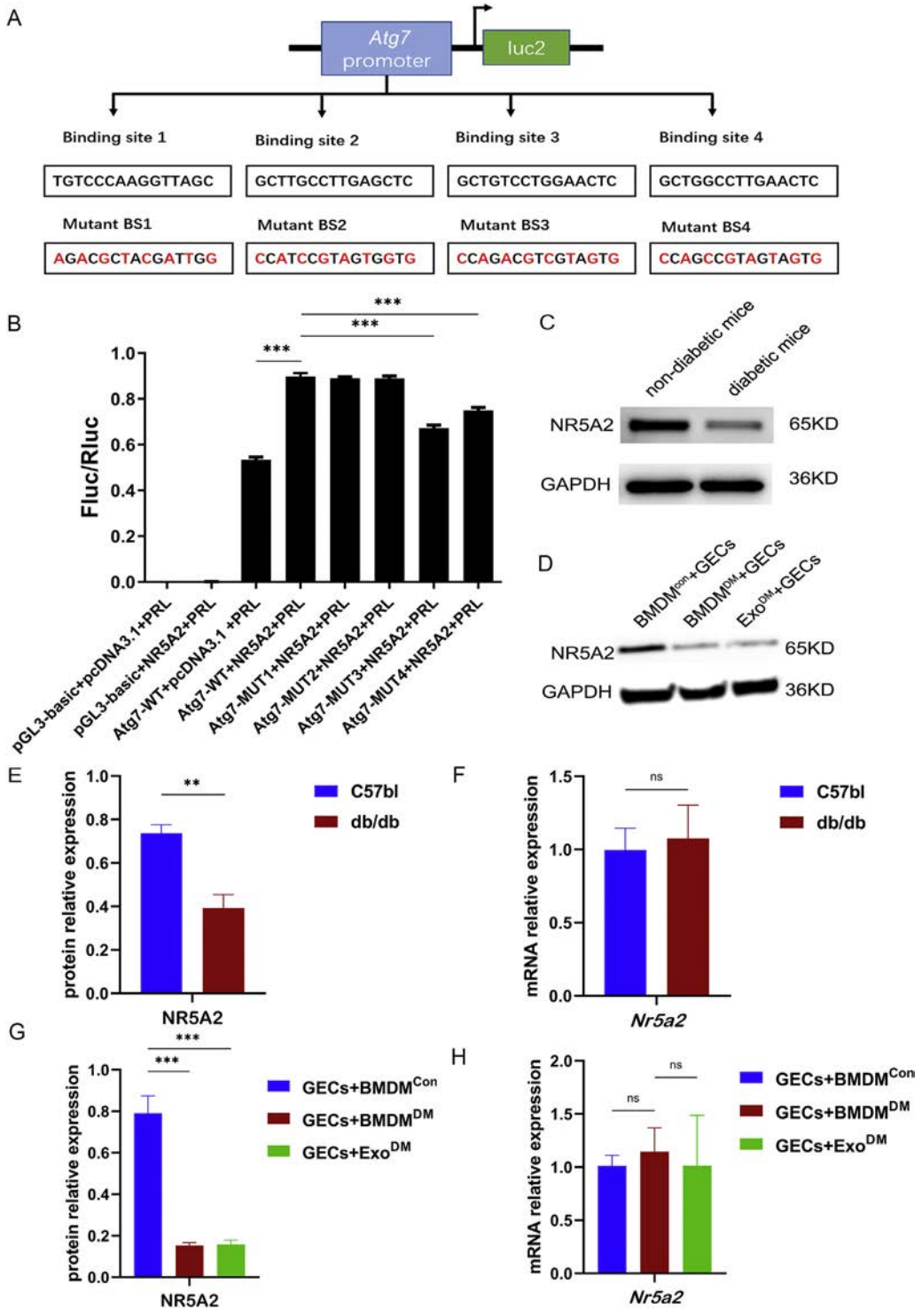

Fig. 2 – NR5A2 is the transcription factor that regulates ATG7 expression in GECs and is inhibited by BMDMs/Exos under diabete conditions. A and B, A dual-luciferase reporter assay was conducted to compare the activities of the WT *Atg7* promoter or the promoter with mutations in binding site 1-4 (MUT1-4) of the NR5A2 binding element. A, Luciferase activity was measured and analysed. B, C, and E, Western blotting was used to analyse NR5A2 expression in nondiabetic mice and diabetic mice), and statistical analysis was performed (E,F) RT–PCR analysis of Nr5a2 mRNA expression in GECs from nondiabetic mice and diabetic mice. D and G, Western blotting was used to analyse NR5A2 expression in GECs after incubation with BMDMs and BMDMs/Exos (D), and statistical analysis was performed (G). H, RT–PCR analysis of Nr5a2 mRNA expression in GECs after incubation with BMDMs and BMDMs/Exos. All the Western blotting and quantitative RT–PCR experiments were repeated three independent times ($n = 3$), $^{*}P < .05$ $^{**}P < .01$ $^{***}P < .001$. The data are shown as the mean ± *s.d.* DM: harvest from db/db mice; Con: harvested from C57BL mice; Exo: exosomes secreted by bone marrow-derived macrophages.

Decreasing NR5A2 activity impairs the autophagic flux and exacerbates inflammation in GECs

To explore the relationship between NR5A2 and autophagic flux, NR5A2-targeting siRNA was utilised to establish a GEC model. Quantitative RT–PCR and Western blotting were performed to measure the expression of *Atg7*, *P62*, and *Lc3b* (LC3-I and LC3-II). The results indicated that the mRNA expressions of *Nlrp3*, *Il1β*, *Lc3b*, *and P62* were significantly upregulated, while *Atg7* was significantly downregulated in GECs transfected with NR5A2-targeting siRNA (Figure 3B). Correspondingly, the protein expressions of NLRP3, IL1β and P62 were significantly increased, while ATG7 and LC3II/I were significantly decreased in GECs transfected with NR5A2-targeting siRNA (Figure 3A,C). These results suggested that downregulation of NR5A2 could inhibit ATG7-dependent autophagy and exacerbate inflammation in GECs.

To further investigate the effects of NR5A2 overexpression on the role of exosomes secreted by BMDMs from db/db mice ($Exos^{DM}$) in disrupting autophagy and exacerbating inflammation in GECs, a NR5A2-overexpressing GEC model ($GECs^{HBLV\text{-}NR5A2}$) was established via lentivirus transfection. After coincubation with $Exos^{DM}$, trends of decreased inflammatory indicator expression (NLRP3 and IL1β) and autophagic substrate accumulation (P62) were observed compared to control vector-introduced GECs ($GECs^{HBLV\text{-}PURO}$). Furthermore, trends of recovery in the levels of autophagic substrate delivery indicators (ATG7 and LC3-II/I) were also observed (Figure 3D-3F). These results indicated that NR5A2 overexpression could partially rescue Exo^{DM}-induced autophagy disruption and prevent Exo^{DM}-mediated inflammation in GECs.

MiR-381-3p levels are significantly elevated in GECs after coculture with BMDMs from diabetic mice

Macrophages are phagocytic cells that play crucial roles in periodontitis by initiating innate immune responses and regulating various stages of inflammation. Three miRNA target databases (TargetScan/miRDB/miRWalk) were applied to identify miRNAs that regulate NR5A2. Subsequently, small RNA sequencing (miR-seq) was used to identify and validate the differentially expressed miRNAs in Exos from the control group ($Exos^{Con}$) and db/db mouse group ($Exos^{DM}$). As a result, 116 miRNAs were identified (absolute expression fold change>2 and $P < .05$) (Supplementary Data S2). A Venn diagram was used to visualise the intersection of database-predicted miRNAs and differentially expressed miRNAs that were identified by small RNA sequencing; the Venn diagram identified 8 miRNAs (Figure 4A). The fold-change values ($Exos^{DM}$ versus $Exos^{Con}$) of these 8 miRNAs according to the small RNA sequencing results are shown in descending order (Figure 4B). After comprehensive bioinformatics analysis and small RNA sequencing data analysis, miR-381-3p was found to be the most significantly upregulated miRNA and was selected for further analysis. To validate the sequencing results, the expression levels of miR-381-3p in GECs that were coincubated with $Exos^{Con}$/$Exos^{DM}$/$Exos^{Con}$+LPS/$Exos^{DM}$+LPS were examined using qRT–PCR, which confirmed that the miR-381-3p expression levels were significantly upregulated in the diabetes groups (Figure 4C).

A double luciferase reporter assay was utilised to assess whether *Nr5a2* mRNA is a target of miR-381-3p. The results showed that miR-381-3p significantly decreased the luciferase activity of WT-Nr5a2 but had no significant effect on the luciferase activity of MUT-Nr5a2 (Figure 4D). This suggests that *Nr5a2* mRNA is a predicted target of miR-381-3p and that these molecules interact at a potential binding site within the 3′-UTR of *Nr5a2* mRNA (Figure 4D,E). These findings indicate that miR-381-3p may be a potential biomarker of exacerbated inflammation in the periodontium of individuals with diabetes.

MiR-381-3p enrichment disrupts the autophagic flux and exacerbates inflammation in GECs by targeting NR5A2

GECs were transfected with a miR-381-3p mimic/inhibitor or negative control (NC) to investigate the function of Exo-derived miR-381-3p. qRT–PCR and Western blotting analyses revealed that miR-381-3p suppresses NR5A2 protein expression in GECs, as the protein expression level of NR5A2 was significantly decreased after miR-381-3p mimic transfection compared with NC transfection (Figure 5A,C). Additionally, the expression of autophagy-related genes (*Atg7*, *P62* and *Lc3b*) and inflammation-related genes (*Nlrp3* and *Il1β*) were analysed. The results showed that the mRNA and protein expression levels of NLRP3, IL1β and P62 were significantly increased and the ATG7 and LC3II/I levels were significantly decreased in miR-381-3p mimic-transfected GECs compared with the NC group (Figure 5A-C). This suggests that miR-381-3p mimic transfection disrupts the autophagic flux and exacerbates inflammation in GECs.

Moreover, the mRNA and protein expression levels of NLRP3, IL1β and P62 were significantly decreased and the ATG7 and LC3II/I levels were significantly increased in the miR-381-3p inhibitor+Exo^{DM} group compared with the Exo^{DM} group (Figure 5D-F). This implies that the miR-381-3p inhibitor reverses the Exo^{DM}-mediated disruption of the autophagy flux and alleviates inflammation in GECs.

Overall, a high-glucose microenvironment exacerbates inflammation in GECs through NR5A2-dependent autophagic flux disruption, and BMDM-derived exosomal miR-381-3p serves as a posttranscriptional negative regulator of NR5A2.

Discussion

The gingival epithelium performs its barrier function in two ways. One is the physical barrier function which is mediated by interconnecting keratinocytes that form bridges between adjacent epithelial cells via cell adhesion molecules (CAMs).[8] The second is the immune homeostasis. To address bacterial challenges, gingiva epithelial cells (GECs) express different kinds of pattern recognition receptors (PRRs) that contribute to the recognition of pathogen-associated molecular patterns (PAMPs).[9–11] In early stages of infection, GECs respond strongly to LPS through its recognition by TLRs, producing cytokines such as IL-6, INF-γ, or TNF-α and causing persistent periodontal inflammation.[12,13] GECs are also considered non-professional phagocytes that actively internalise pathogens in an opsonization-independent manner.[14] Periodontal

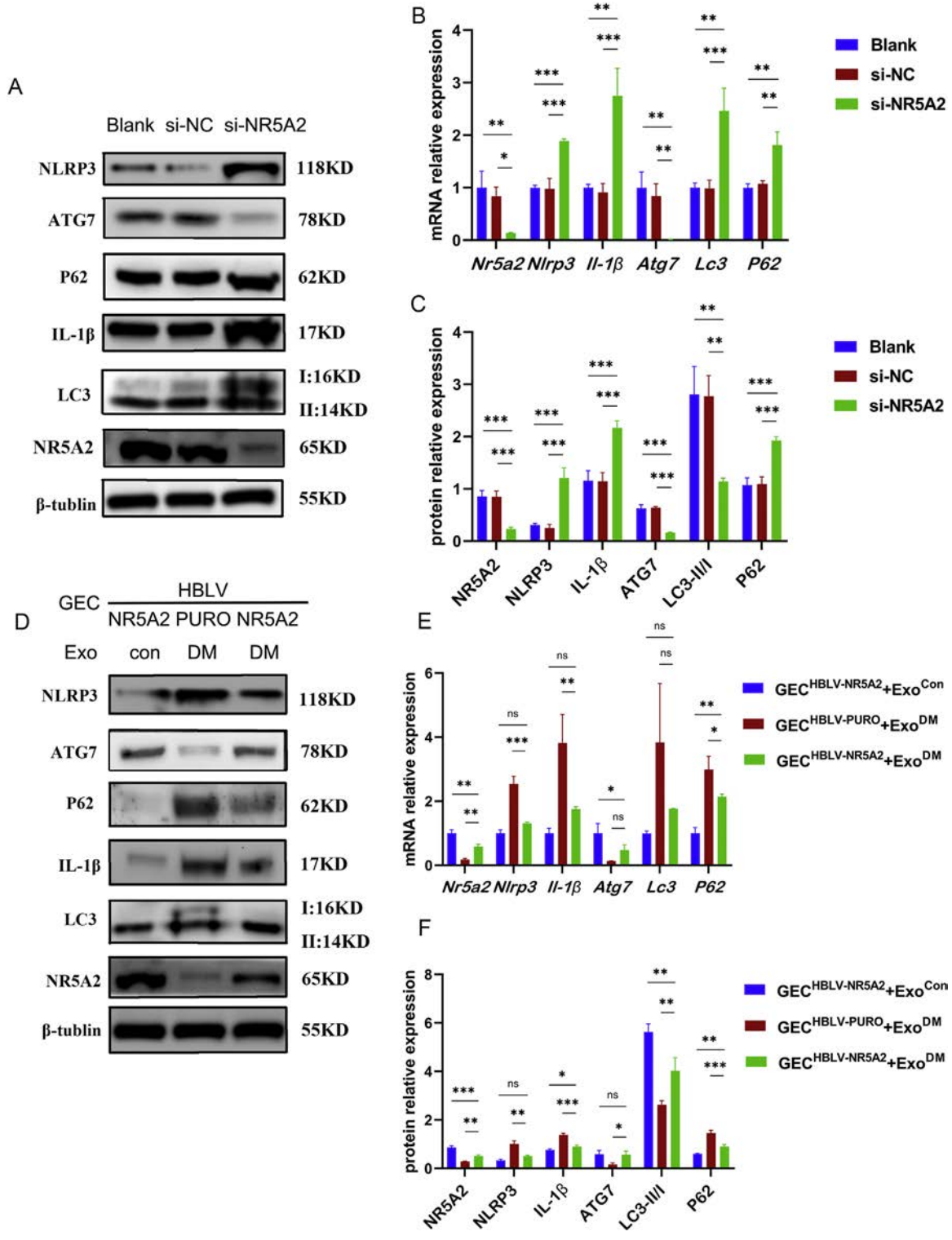

Fig. 3 – The effect of NR5A2 expression on the autophagy flux and inflammation level in GECs. A and C, Western blotting analysis of the autophagic flux and inflammation levels in GECs after si-NR5A2 transfection (A), and statistical analysis was performed (C). B, The autophagy flux (autophagy genes: *Atg7*, *Lc3b*, and *p62*), inflammation levels (inflammatory genes: *Nlrp3* and *Il-1β*), and Nr5a2 mRNA expression in GECs was analysed after si-NR5A2 transfection. D and F, Western blotting was used to analyse the autophagic flux and inflammation levels in GECs to verify the rescue effect of NR5A2 overexpression through lentiviral transduction (D), and statistical analysis was performed (F). E, qRT–PCR analysis of the autophagy flux (autophagy genes: *Atg7*, *Lc3b*, and *p62*), inflammation levels (inflammatory genes: *Nlrp3*and *Il-1β*) and Nr5a2 mRNA expression in GECs after NR5A2 overexpression through lentiviral transduction. All the Western blotting and quantitative RT–PCR experiments were repeated three independent times ($n = 3$), $^{*}P < 005$ $^{**}P < .01$ $^{***}P < .001$. The data are shown as the mean ± *s.d.* DM: harvested from db/db mice; Con: harvested from C57BL mice; Exo: exosomes secreted by bone marrow-derived macrophages.

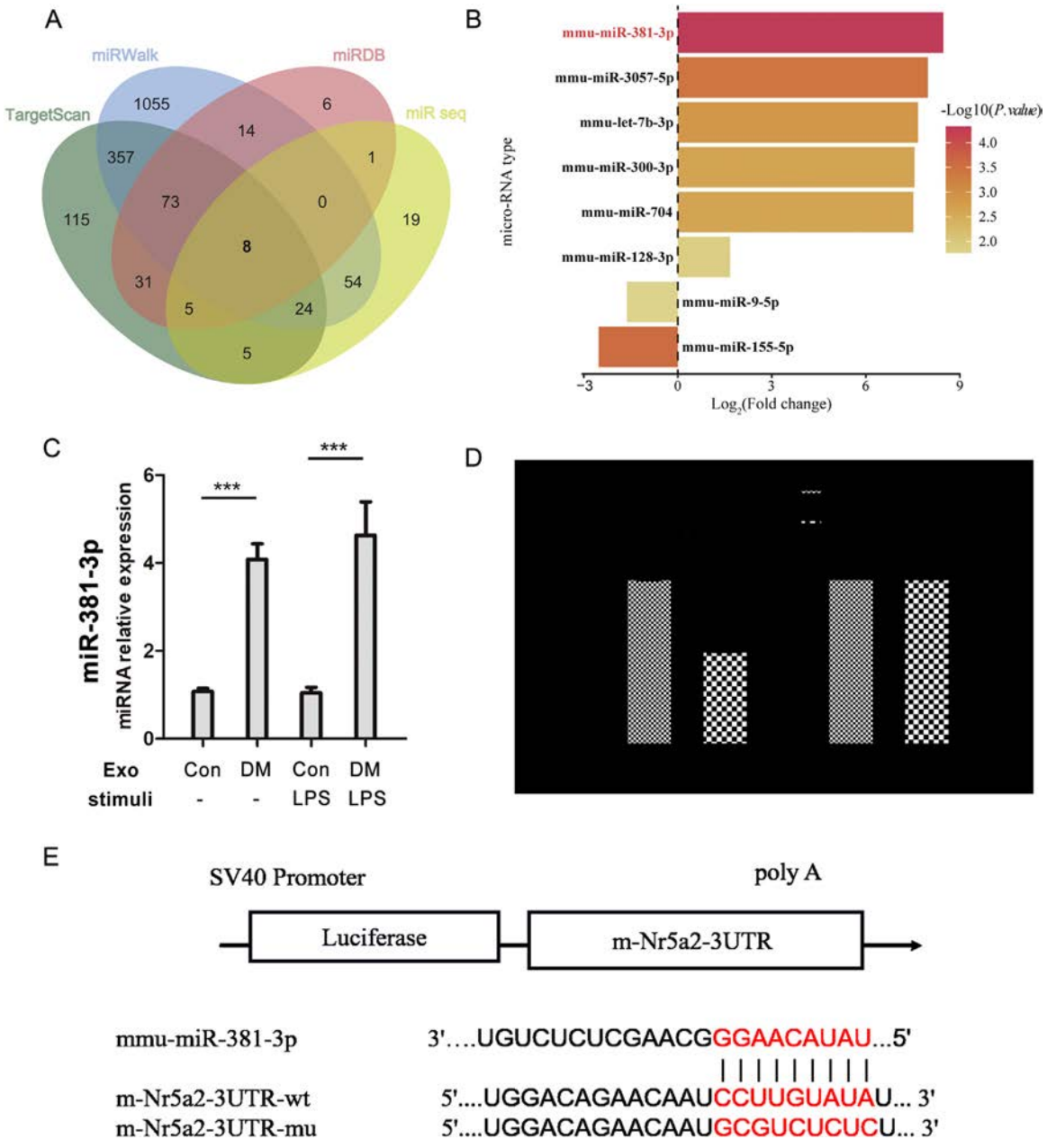

Fig. 4 – MiR-381-3p is the most prominent miRNA that targets Nr5a2 in GECs. A, Venn diagram showing the intersection of miRNAs that were predicted with three databases (TargetScan/miRDB/miRWalk) and differentially expressed miRNAs that were identified by miRNA sequencing (comparing gingival tissue from db/db mice and C57BL mice). B, Ranked bar graph shows the log2-fold change in the expression of 8 overlapping miRNAs according to miRNA sequencing datasets, with downregulation shown as negative values and upregulation as positive values. Mmu-miR-381-3p had the most significant and highest fold change. C, qRT–PCR validation of miR-381-3p expression in BMDMs/Exos (nondiabetic mice and diabetic mice) in the presence or absence of Pg-LPS. D, Luciferase assay was used to analyse the interaction between miR-381-3p and the 3'-UTR of Nr5a2 mRNA. E) Predicted miR-381-3p target sequences in the 3'-UTR of Nr5a2 mRNA (m-Nr5a2-3UTR-wt) and sequence after mutations were made in the 3'-UTR of Nr5a2 mRNA (m-Nr5a2-3UTR-mu). All the Western blotting and quantitative RT–PCR experiments were repeated three independent times ($n = 3$), $^{*}P < .05$ $^{**}P < .01$ $^{***}P < .001$. The data are shown as the mean ± s.d. DM: harvested from db/db mice; Con: harvested from C57BL mice; Exo: exosomes secreted by bone marrow-derived macrophages; Pg: *Porphyromonas gingivalis*.

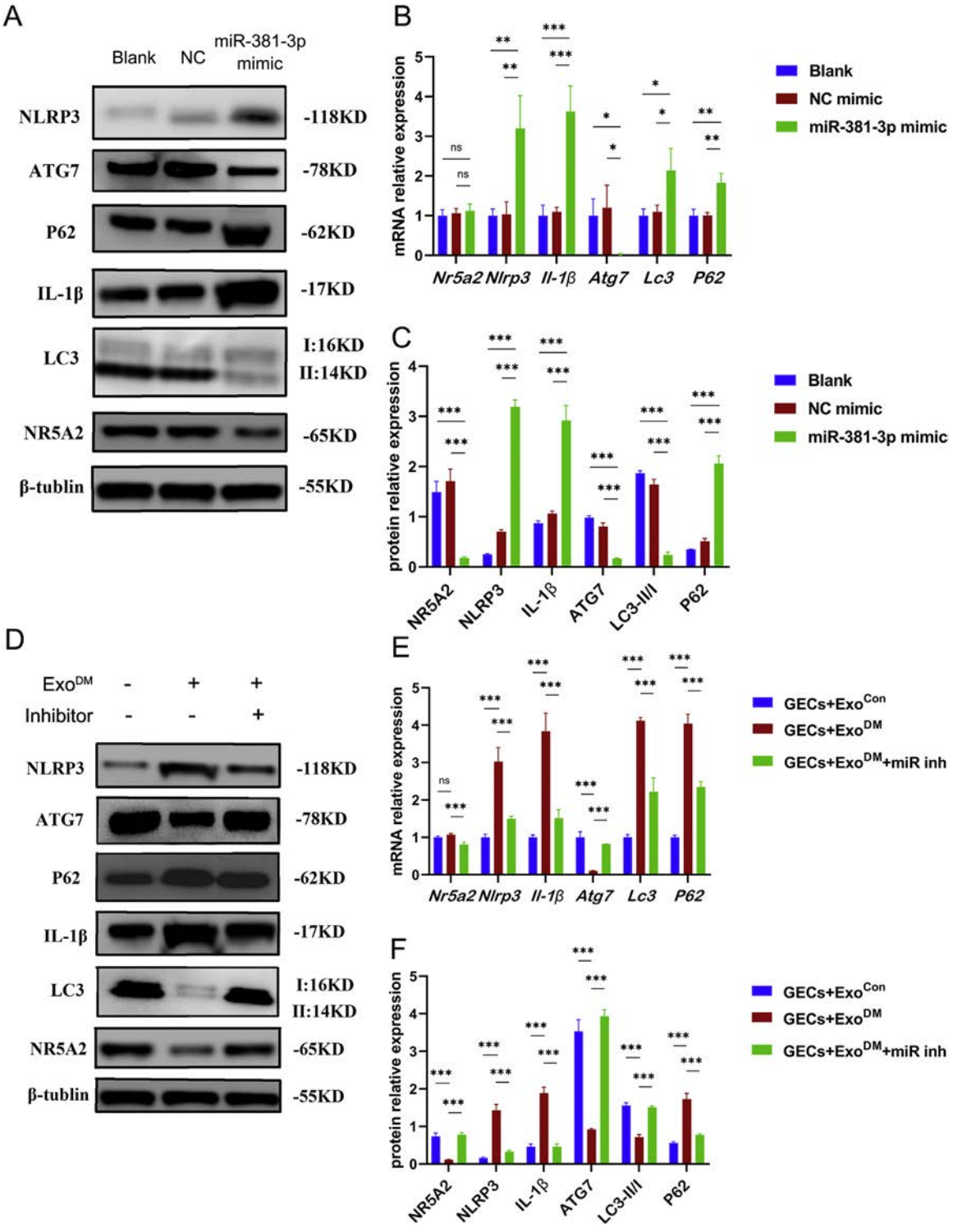

Fig. 5 – The effect of miR-381-3p expression on the autophagic flux and inflammation level in GECs. A and C, Western blotting analysis of the autophagic flux and inflammation levels in GEC after miR-381-3p mimic transfection (A), and statistical analysis was performed (C). B, qRT–PCR analysis of the autophagy flux (autophagy genes: *Atg7*, *Lc3b*, and *p62*), inflammation levels (inflammatory genes: *Nlrp3* and *Il-1β*) and Nr5a2 mRNA expression in GECs after miR-381-3p mimic transfection. D and F, Western blotting was used to analyse the autophagy flux and inflammation levels in GECs to verify the rescue effect in GECs after incubation with BMDMs/Exos from diabetic mice after miR-381-3p inhibitor transfection (D), and statistical analysis was performed (F). E) qRT–PCR analysis of the autophagy flux (autophagy genes: *Atg7*, *Lc3b*, and *p62*), inflammation levels (inflammatory genes: *Nlrp3*and *Il-1β*) and Nr5a2 mRNA expression in GECs after miR-381-3p inhibitor transfection. All the Western blotting and quantitative RT–PCR experiments were repeated three independent times ($n = 3$), $^{*}P < .05$ $^{**}P < .01$ $^{***}P < .001$. The data are shown as the mean ± s.d. DM: harvested from db/db mice; Con: harvested from C57BL mice; Exo: exosomes secreted by bone marrow-derived macrophages; miR inh: miR-381-3p inhibitor

pathogens may cross epithelial barriers, get access to internal tissues and survive under the impaired barrier function, leading to severe periodontitis. However, the detail mechanism is still unclear.

Autophagy, orchestrated by the interplay of autophagy-related (ATG) proteins, including ATG3 and ATG7, is responsible for the degradation of cytoplasmic contents such as proteins and organelles.[15] Furthermore, a connection between autophagy and phagocytosis exists through LC3-associated phagocytosis (LAP), observed in both professional and non-professional phagocytes, including gingival epithelial cells (GECs).[16] As a critical component of epithelial cell defense mechanisms, autophagy contributes significantly to the innate immune response against antigens. However, the impact of autophagy on intracellular bacteria varies based on their stage and state, particularly under inflammatory and non-inflammatory conditions.

Under normal circumstances, autophagy acts protectively against bacteria by directing them to autophagosomes, which subsequently fuse with lysosomes.[17] Nevertheless, certain intracellular bacteria, such as *Porphyromonas gingivalis* (*P. gingivalis*), have evolved strategies to manipulate autophagy, disrupting host defense mechanisms and persisting within GECs. Under such conditions, autophagosomes serve as an additional mechanism by which bacteria target and escape immune surveillance.[18] *P. gingivalis*, recognised as the keystone pathogen of periodontitis, specifically binds to Beta-1 integrins in gingival epithelial cells, facilitating invasion.[19] Upon internalization, *P. gingivalis* localises to endoplasmic reticulum (ER)-rich regions, promoting LC3 lipidation and phagophore formation. Facilitating autophagy supports *P. gingivalis* entry into GECs, enables colonization within autophagosomes, and aids in evading the binding of antimicrobial proteins NDP52 and p62, ultimately escaping lysosomal degradation.[20] In later stages of autophagy, *P. gingivalis* promotes its long-term survival within GECs by facilitating lysosomal efflux and inhibiting autophagosome-lysosome fusion. Additionally, autophagy plays a role in both cytokine production and elimination, contributing to the preservation of balanced immune responses amidst inflammation.

The progression of diabetes often coincides with a chronic systemic inflammatory state.[21] Enhanced autophagy, as indicated by the upregulation of numerous ATG proteins during periodontal inflammation, suggests a protective role against inflammation to some extent.[22] However, impaired autophagy has been observed in keratinocytes, BMDMs, and endothelial cells under high glucose conditions, affecting cell viability and function.[23,24] Our study reveals impaired barrier function in GECs of individuals with diabetes, manifested by the inhibition of intracellular autophagy and an exacerbation of the inflammatory response.

Among autophagy-related (ATG) genes, ATG3 and ATG7 are two of the most important regulators that mediate LC3 maturation and switching.[25] However, significant differences were observed in the mRNA and protein expressions of ATG7 but not ATG3 in our study, indicating that ATG7 may play a key role in this autophagy flux disruption. To investigate the upstream regulatory molecules of ATG7, the Animal TFDB database (v. 3.0) was introduced to identify the most relevant transcription factor that regulates ATG7 expression. Eventually, NR5A2 was identified and was successfully confirmed in subsequent dual-luciferase reporter assays.

Macrophages play pivotal roles in orchestrating the immune response during periodontal inflammation.[26] It was reported that macrophages can regulate epithelial function through extracellular vehicles (EVs);[4,27–29] EVs carry miRNA molecules, which were proven to participate in the progression of atherosclerosis and attenuation of pulmonary fibrosis through macrophage-epithelial cell/endothelial cell interactions.[30,31] Differential expression of miRNAs in macrophage Exos was reported to occur through the NF-κB/JAK-STAT signalling pathway under high glucose conditions. To determine whether BMDMs disrupt the autophagic flux of GECs, BMDM/Exo+GEC coculture systems were established to investigate the changes in the autophagy flux in GECs; the results proved that BMDMs from diabetic mice could disrupt the autophagy flux and exacerbate inflammation in GECs in an Exo transmission-dependent manner. An increasing number of noncoding RNAs have been also reported to regulate ATG expression.[32] Finally, three miRNA target databases (TargetScan/miRDB/miRWalk) were used to predict relevant miRNAs, and these results were combined with the BMDM exos RNA-seq results of db/db and control mice. MiR-381-3p was proven to be the key molecule that bridges the interaction between macrophages and GECs under diabetes conditions.

NR5A2, which is also known as liver receptor homolog-1 (LRH-1), was identified early as a regulator of intracellular cholesterol homeostasis.[33] It was previously demonstrated that NR5A2 is expressed in pancreatic islets, which play an important role in the maintenance of glucose homeostasis.[34] Among the various regulatory modalities, transcriptional and posttranslational regulation is thought to be the most likely mechanism of regulation.[35] In our study, miR-381-3p was proven to downregulate NR5A2 expression, which is consistent with our previous suggestion. Recently, NR5A2 was widely studied as a potential target for treating diabetes mellitus. Research has demonstrated that NR5A2 agonism effectively prevents pancreatic β-cell apoptosis and alleviates immune-dependent inflammation of the pancreas.[33] We discovered that NR5A2 plays an important role in the pathogenesis of diabetic periodontitis. Therefore, NR5A2 may be a promising therapeutic target for enhancing epithelial barrier function in diabetic periodontitis.

In this study, we revealed impaired communication between the gingival epithelial cells and macrophages through exosomal miRNAs in diabetic individuals, and these results provided new ideas and targets for the clinical application of therapeutic vesicles or specific miRNAs to reverse diabetic periodontitis. However, no specific subtypes of macrophage were examined in our study, resulting in some limitations in this study. Whether the selective loading of miRNAs into vesicles achieved related to the polarization or senescence of macrophages under diabetic conditions needs to be further explored.

Conclusion

Our research represents an innovative study of the epithelium barrier, confirming the effect of macrophage-epithelial

cell interactions in exacerbating inflammation. Additionally, the mechanism of NR5A2 regulation was discovered, providing a theoretical basis for further study of periodontal innate immunity. This study may contribute to the screening of related therapeutic targets in diabetic periodontitis and developing relevant drugs.

Data availability statement

The datasets used and/or analysed during the current study are available from the corresponding author upon reasonable request.

Author contributions

X.H. and M.L. designed the project. Y.Z. and S.K. collected the data, L.W., X.H. and H.L. wrote the main manuscript text and prepared figures. L.W. and Z.S. completed the data analysis. Z.L. and X.H. obtained financial support. All authors reviewed the manuscript.

Funding

This work was supported by the National Natural Science Foundation of China (Grant Numbers 82201056, 82170939), National Natural Science Foundation of China-Guangdong Joint Fund (Grant Numbers U22A20157) and the Natural Science Foundation of Guangdong Province, China (Grant Number 2022A1515012343).

Conflict of interest

The authors have no conflicts of interest related to this article.

Acknowledgements

Special thanks to Fangcao Lei for bioinformatic support and Chaoye Wang for technical help.

Supplementary materials

Supplementary material associated with this article can be found in the online version at doi:10.1016/j.identj.2024.02.001.

REFERENCES

1. IDF DIABETES ATLAS [Internet]. 10th edition. Brussels: International Diabetes Federation; 2021. Available from: https://www.ncbi.nlm.nih.gov/books/NBK581934/
2. Klionsky DJ, Abeliovich H, Agostinis P, et al. Guidelines for the use and interpretation of assays for monitoring autophagy in higher eukaryotes. Autophagy 2008;4(2):151–75.
3. Okabe Y, Medzhitov R. Tissue-specific signals control reversible program of localization and functional polarization of macrophages. Cell 2014;157(4):832–44.
4. Han CZ, Juncadella IJ, Kinchen JM, et al. Macrophages redirect phagocytosis by non-professional phagocytes and influence inflammation. Nature 2016;539(7630):570–4.
5. Xu Z, Zeng S, Gong Z, Yan Y. Exosome-based immunotherapy: a promising approach for cancer treatment. Mol Cancer 2020;19(1):160.
6. Shimoe M, Yamamoto T, Shiomi N, Tomikawa K, Hongo S, Yamashiro K, et al. Overexpression of smad2 inhibits proliferation of gingival epithelial cells. J Periodontal Res 2014;49(3):290–8.
7. Shen Z, Kuang S, Zhang M, Huang X, Chen J, Guan M, et al. Inhibition of Ccl2 by bindarit alleviates diabetes-associated periodontitis by suppressing inflammatory monocyte infiltration and altering macrophage properties. Cell Mol Immunol 2021;18(9):2224–35.
8. Groeger SE, Meyle J. Epithelial barrier and oral bacterial infection. Periodontol 2000 2015;69(1):46–67.
9. Medzhitov R. Innate immunity: quo vadis? Nat Immunol 2010;11(7):551–3.
10. Medzhitov R. Inflammation 2010: new adventures of an old flame. Cell 2010;140(6):771–6.
11. Meyle J, Dommisch H, Groeger S, Giacaman RA, Costalonga M, Herzberg M. The innate host response in caries and periodontitis. J Clin Periodontol 2017;44(12):1215–25.
12. Kocgozlu L, Elkaim R, Tenenbaum H, Werner S. Variable cell responses to *P. Gingivalis* lipopolysaccharide. J Dent Res 2009;88(8):741–5.
13. Herath TD, Darveau RP, Seneviratne CJ, Wang CY, Wang Y, Jin L. Tetra- and penta-acylated lipid a structures of *Porphyromonas Gingivalis* Lps differentially activate Tlr4-mediated Nf-kappab signal transduction cascade and immuno-inflammatory response in human gingival fibroblasts. PLoS One 2013;8(3):e58496.
14. Ribet D, Cossart P. How bacterial pathogens colonize their hosts and invade deeper tissues. Microbes Infect 2015;17(3):173–83.
15. Mauthe M, Langereis M, Jung J, et al. An sirna screen for Atg protein depletion reveals the extent of the unconventional functions of the autophagy proteome in virus replication. J Cell Biol 2016;214(5):619–35.
16. Heckmann BL, Boada-Romero E, Cunha LD, Magne J, Green DR. Lc3-associated phagocytosis and inflammation. J Mol Biol 2017;429(23):3561–76.
17. Gomes LC, Dikic I. Autophagy in antimicrobial immunity. Mol Cell 2014;54(2):224–33.
18. Buratta S, Tancini B, Sagini K, et al. Lysosomal exocytosis, exosome release and secretory autophagy: the autophagic- and endo-lysosomal systems go extracellular. Int J Mol Sci 2020;21(7).
19. Lee Kyulim, Roberts JoAnn S, Choi Chul Hee, Atanasova Kalina R, Yilmaz Özlem. *Porphyromonas Gingivalis* traffics into endoplasmic reticulum-rich-autophagosomes for successful survival in human gingival epithelial cells. Virulence 2018;9(1):845–59.
20. Liu M, Shao J, Zhao Y, Ma B, Ge S. *Porphyromonas Gingivalis* evades immune clearance by regulating lysosome efflux. J Dental Res 2023;102(5):555–64.
21. Zhou XY, Zhang F, Hu XT, et al. Depression can be prevented by astaxanthin through inhibition of hippocampal inflammation in diabetic mice. Brain Res 2017;1657:262–8.
22. Ebersole JL, Kirakodu SS, Neumann E, Orraca L, Martinez JGonzalez, Gonzalez OA. Oral microbiome and gingival tissue apoptosis and autophagy transcriptomics. Front Immunol 2020;11:585414.
23. Li L, Zhang J, Zhang Q, et al. High glucose suppresses keratinocyte migration through the inhibition of P38 Mapk/autophagy pathway. Front Physiol 2019;10:24.
24. Zhang PW, Tian C, Xu FY, et al. Green tea polyphenols alleviate autophagy inhibition induced by high glucose in endothelial cells. Biomed Environ Sci 2016;29(7):524–8.
25. Fang S, Su J, Liang B, et al. Suppression of autophagy by mycophenolic acid contributes to inhibition of HCV replication in human hepatoma cells. Sci Rep 2017;7:44039.

26. Qian SJ, Huang QR, Chen RY, et al. Single-cell RNA sequencing identifies new inflammation-promoting cell subsets in Asian patients with chronic periodontitis. Front Immunol 2021;12:711337.
27. Freeman SA, Grinstein S. Phagocytosis: how macrophages tune their non-professional counterparts. Curr Biol 2016;26 (24):R1279–R82.
28. Spalinger Marianne R, Sayoc-Becerra Anica, Santos Alina N, et al. Ptpn2 regulates interactions between macrophages and intestinal epithelial cells to promote intestinal barrier function. Gastroenterology 2020;159(5):1763–1777.e14.
29. Hu Q, Lyon CJ, Fletcher JK, Tang W, Wan M, Hu TY. Extracellular vesicle activities regulating macrophage- and tissue-mediated injury and repair responses. Acta Pharm Sin B 2021;11 (6):1493–512.
30. Wang Y, Xu Z, Wang X, et al. Extracellular-vesicle containing mirna-503-5p released by macrophages contributes to atherosclerosis. Aging (Albany NY) 2021;13(8):12239–57.
31. Kishore A, Petrek M. Roles of macrophage polarization and macrophage-derived miRNAs in pulmonary fibrosis. Front Immunol 2021;12:678457.
32. Zhao Y, Wang Z, Zhang W, Zhang L. Non-coding RNAs regulate autophagy process via influencing the expression of associated protein. Prog Biophys Mol Biol 2020;151:32–9.
33. Sun Y, Demagny H, Schoonjans K. Emerging functions of the nuclear receptor Lrh-1 in liver physiology and pathology. Biochim Biophys Acta Mol Basis Dis 2021;1867(8):166145.
34. Martin Vazquez E, Cobo-Vuilleumier N, Araujo Legido R, et al. Nr5a2/Lrh-1 regulates the Ptgs2-Pge(2)-Ptger1 pathway contributing to pancreatic islet survival and function. iScience 2022;25(5):104345.
35. Meinsohn MC, Smith OE, Bertolin K, Murphy BD. The orphan nuclear receptors steroidogenic factor-1 and liver receptor homolog-1: structure, regulation, and essential roles in mammalian reproduction. Physiol Rev 2019;99 (2):1249–79.